Available online at www.sciencedirect.com
ScienceDirect
International Journal of Heat and Mass Transfer 51 (2008) 361–377
International Journal of HEAT and MASS TRANSFER
www.elsevier.com/locate/ijhmt

Variation of population inversion and gain characteristics with D_2 injection angle in DF chemical laser cavity

Jun Sung Park [a,*], Seung Wook Baek [a], Doyoung Byun [b]

[a] Division of Aerospace Engineering, Department of Mechanical Engineering, Korea Advanced Institute of Science and Technology, 373-1 Guseong-dong, Yuseong-gu, Daejeon 305-701, Republic of Korea
[b] Department of Aerospace Engineering, Konkuk University, 1 Hwayang-Dong, Kwangjin-Gu, Seoul 143-701, Republic of Korea

Received 15 January 2007; received in revised form 19 September 2007
Available online 3 December 2007

Abstract

Nowadays, a chemical laser has been developed not only for a strategic military purpose, but also as a manufacturing tool in industrial usage due to its high power lasing characteristics. In order to increase the laser beam power in the chemical laser systems, the mixing efficiency of fuel and oxidant should be improved, since more excited molecules are followed by high mixing efficiency. Basically, the production of a lot of excited molecules in the laser cavity results from the high mass flow rates of fuel and oxidant based on efficient mixing and chemical reaction. Therefore, in order to supply higher mass flow to the chemical laser cavity, a radial-expansion nozzle array was used and examined here, not a planar nozzle array which has been widely employed until now. The laser beam generation in this system is achieved by mixing F atoms from supersonic nozzle with D_2 molecules ejecting from holes of round-bended supply lines which are distributed in zigzag configuration, which would extend the reaction zone. Consequently, more excited molecules are expected to be produced, so the intensity of population inversion will be higher.

Since the two-stream injection angle was considered to influence the performance of supersonic combustor, the effects of D_2 injection angles against the main F flow on mixing enhancement, population inversion and gain characteristics were numerically investigated in this study. The results were discussed by comparison with three cases of D_2 injection angles such as 10°, 20° and 40° against the main flow direction. As the injection angle increases, two counter-balancing effects were observed.
© 2007 Elsevier Ltd. All rights reserved.

Keywords: DF chemical laser; Population inversion; Gain; Injection angle; Supersonic combustor

1. Introduction

A chemical laser is known to employ a chemical reaction to produce a population inversion and to offer the possibility of operation without any electrical input. All the energy required for lasing can be produced in the chemical reaction in which D_2 molecule reacts with atomic fluorine. Therefore, a mixing process of one species with another in the chemical laser is so important as to produce excited atoms or molecules, eventually the population inversion occurs.

The mixing process in the chemical laser used to mainly depend on such parameters as pressure ratio of injector to supersonic nozzle [1], species compositions [2,3] and geometric designs [4]. Among them, it is very difficult to change the geometric design parameters in experiments, so that the numerical simulation is likely to play a significant role in this regard. In the chemical laser, the supersonic mixing and its subsequent chemical reaction take place. Consequently, an enhancement in mixing rate is highly desirable. In this respect, the injection or colliding angle of two species is one of the most important factors to affect mixing rate and reaction efficiency [5,6]. By the same reasoning, the angle of injection of D_2 molecules and F atoms in DF chemical laser system is expected to make considerable effects on population inversion.

* Corresponding author. Tel.: +82 42 869 3714; fax: +82 42 869 3710.
E-mail address: jimmy@kaist.ac.kr (J.S. Park).

0017-9310/$ - see front matter © 2007 Elsevier Ltd. All rights reserved.
doi:10.1016/j.ijheatmasstransfer.2007.10.003

Nomenclature

c	speed of light (2.99792458×10^8 m/s)
C_i	mass concentration of ith species (kg/m^3)
C_{pi}	specific heat at constant pressure of ith species (J/kg K)
E, F, G	inviscid flux vectors
E_v, F_v, G_v	viscous flux vectors
e_i	internal energy of ith species (J/kg)
e_t	total internal energy (J/kg)
h_i	enthalpy of ith species (J/kg)
I	intensity (W/m^2)
J	Jacobian
k	thermal conductivity (J/m K s)
M	Mach number
n_i	ith species molar concentration (mol/m^3)
N_A	Avogadro number (mol^{-1})
P	mixture pressure (Pa)
Q	conservative state vector
R_u	universal gas constant (J/kmol K)
S	source vector
T	temperature (K)
t	time (s)
u, v, w	velocities (m/s)
x, y, z	Cartesian coordinates (m)
Y_i	ith species mass fraction
W_i	ith species molecular weight (kg/kmol)

Greek symbols

α	gain coefficient (cm^{-1})
ξ, η, ζ	generalized curvilinear coordinates
$\hbar$	Planck's constant ($6.6260755 \times 10^{-34}$ J s)
κ	Boltzmann constant (5.670×10^{-8} W/m^2 K^4)
ρ	density (kg/m^3)
τ_{ij}	stress tensor
v	transition frequency (s^{-1})
ω	transition frequency, v/c (cm^{-1})

Subscripts

i, j, k	space indices
J	rotational quantum number
ref	reference state
v	vibrational quantum number

Superscript

–	non-dimensional quantities

The laser cavity, which is located in chemical laser, comprises mirrors and injectors of chemical species. In order to generate high lasing power, it is necessary to supply larger amount of chemical species through nozzles. However it is difficult to fabricate many injection holes on the nozzle base enough to supply high mass flow rate. In order to meet these requirements, nowadays, the radial-expansion nozzle array system has been developed and used.

As explained above, the most important factor in designing the radial type nozzle block is a mixing enhancement so as to increase the power of the chemical laser beam. Therefore, in the present study, the population inversion and gain characteristics, which are directly related to the rate of mixing and laser power in this laser system, are numerically studied with a variation of injection angles as one of the important geometric design parameters.

There are lots of numerical and experimental studies regarding the chemical laser. Galaev et al. [7] described the dependence of output power of a CW chemical HF laser with an inhomogeneous distribution of small-signal gain in the active medium on the reflection coefficient of output mirror in the cavity. Also a numerical and experimental method was developed for determination of the properties of active media of lasers, and was applied to determine the energy and amplifying characteristics of a compact HF laser with a radial-expansion nozzle array and to predict the parameters of a large-scale laser. A simple model for a steady flow HF chemical laser was formulated by Broadwell [8], in which the excited state formation rate was limited by the H_2–F mixing rate. However, its simple analytic prediction for lasers was markedly different from the experimental observations. The flow field experiments on a DF chemical laser were conducted by Driscoll and Tregay [9]. The data on the reaction zone structure for laminar mixing were obtained when the mixing was augmented by the gas jet injection at the reactant interface. An experimental investigation was made of the operational characteristics of a self-contained supersonic CW chemical HF laser by Galaev et al. [10], which used a three-jet array with reagent jets spatially separated by helium jets. It was revealed that this type of nozzle array increased the energy characteristics of the laser by a factor of 1.20–1.35 and the length of the active medium by a factor of 1.4–1.7, and at the same time reduced the level of optical inhomogeneity by 30%.

Unlike other laser systems such as solid state laser, semiconductor laser, organic dye laser, etc., the power of chemical laser is predominantly determined by the rate of mixing. Therefore, the optimal conditions, which make it higher and the laser beam more intense, should be sought for improving the chemical laser performance.

In this study, the dependence of population inversion and gain characteristics on variations of D_2 injection angles was numerically investigated in a DF chemical laser cavity in view of the mixing and beam power enhancement. The selected injection angles were 10°, 20° and 40° against the main flow direction. In order to predict chemical as well as thermo-chemical flow development, the governing equa-

tions were non-dimensionalized. And the fully conservative implicit and second-order TVD schemes were used with the finite volume method (FVM). An 11-species (including DF molecules at various excited states of energies), 32-step chemistry model was adopted for the DF reaction to describe the generation and degeneration of the DF excited molecules.

2. Governing equations

The DF chemical laser system considered in the current paper is illustrated in Fig. 1, which shows a radial-expansion nozzle array block. A region, which is indicated by dot lines, is a computational domain where the effects of injection angles on mixing enhancement and population inversion are numerically examined. It consists of a partial section of the entire radial-expansion nozzle, a part of the round-bended D_2 supply line, the D_2 injection holes and the cavity. A detailed cross-section view of the D_2 supply line with the D_2 injection holes is presented in the upper right side of Fig. 1.

Through the radial-expansion nozzle, the uniform mixture of F, F_2, HF and He radially flows into the DF chemical laser cavity at $M = 4.5$, $P = 7.49$ Torr and $T = 275.86$ K as indicated in Fig. 1. And, from the D_2 injection hole, the D_2 molecules are injected at $M = 1$, $P = 200.96$ Torr and $T = 250.35$ K. The injection angles against the main flow direction considered in this study are 10°, 20° and 40°, respectively. The D_2 injection holes in each of the upper and lower round-bended D_2 supply lines are positioned in a staggered way. The reason is that this type of injection positioning makes mixing (surface) area even wider for more efficient mixing.

In order to analyze these phenomena in the domain explained above, three-dimensional full Navier–Stokes equations and species conservation equations are applied to a section of the radial-expansion nozzle block. Also the gain coefficients are calculated under the assumption of the equilibrium Boltzmann distribution for the rota-

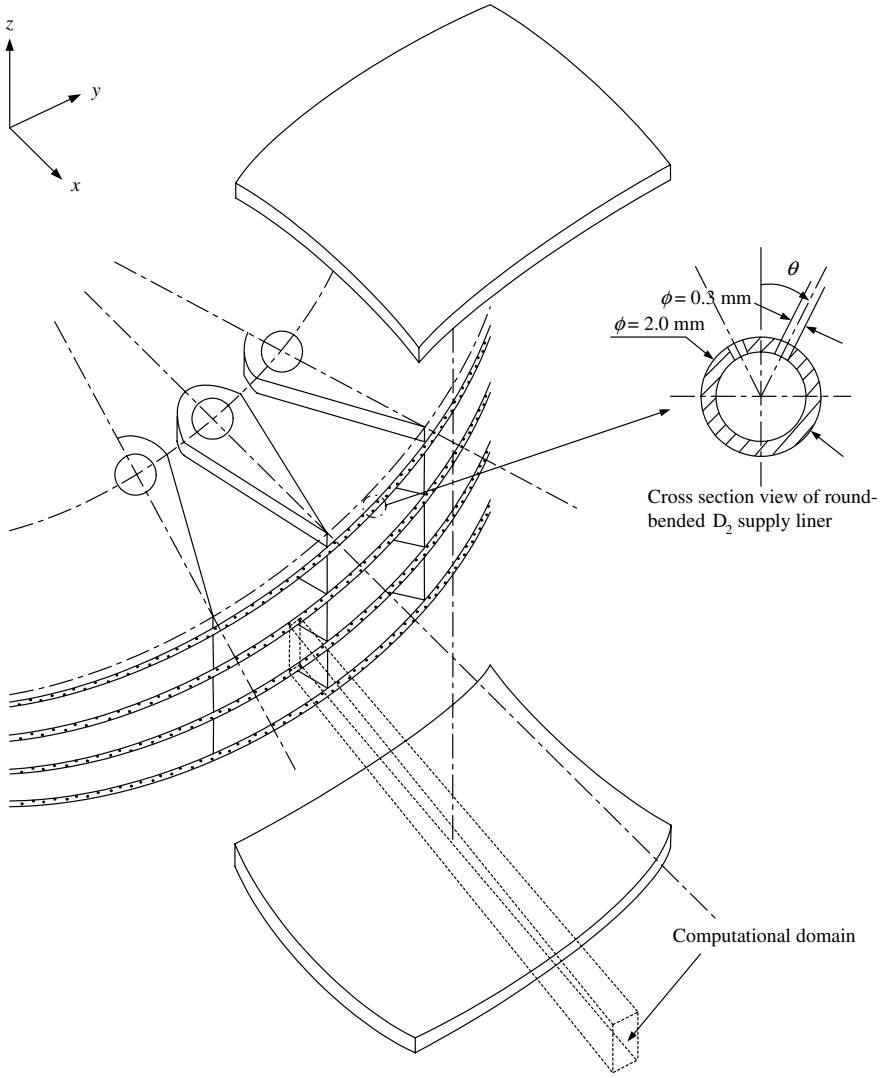

Fig. 1. Schematic of a DF chemical laser cavity block with a radial-expansion nozzle array.

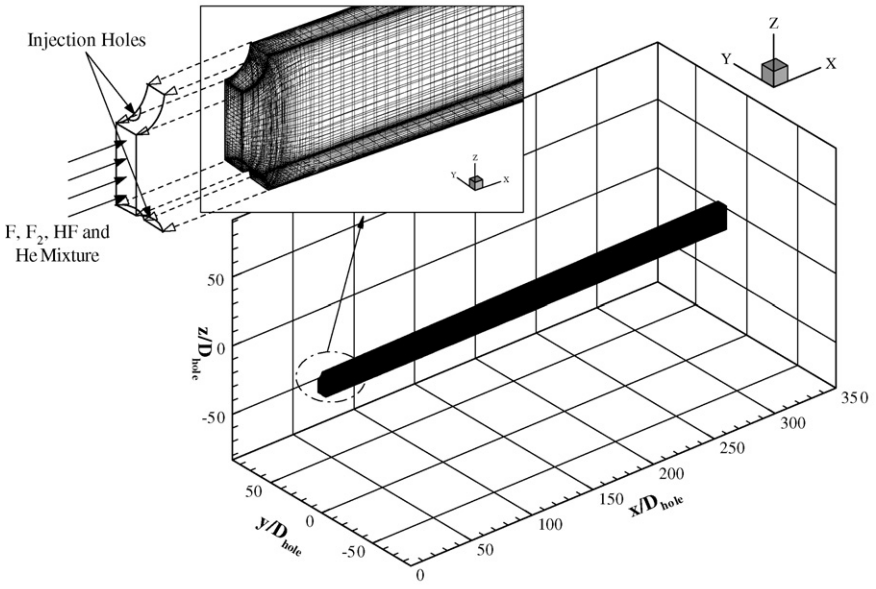

Fig. 2. Grid system for a section of the DF chemical laser cavity block.

tional populations at the translational temperature T. The rotational energy states for each vibrational state are indicated by

$$\rho_{v,J} = \rho_v \frac{2J+1}{Q(v)} \exp\left(-\frac{\hbar c}{k}\frac{E_{v,J}}{T}\right), \tag{1}$$

where $Q(v)$ is the rotational-partition function for a vibrational level v, c is the speed of light, κ is the Boltzmann constant, and $E_{v,J}$ is the rotational energy of state v, J.

2.1. Governing equations

Among the equations used to describe a three-dimensional chemical laser system are the time-dependent compressible full Navier–Stokes equations with the detailed chemical reaction mechanism. The entire system of equations is cast in the following form:

$$\frac{\partial Q}{\partial t} + \frac{\partial E}{\partial x} + \frac{\partial F}{\partial y} + \frac{\partial G}{\partial z} = \frac{\partial E_v}{\partial x} + \frac{\partial F_v}{\partial y} + \frac{\partial G_v}{\partial z} + S_{\text{chem}}, \tag{2}$$

where Q is the conservative flow variable vector, and E, F and G are the inviscid flux vectors in the x, y and z directions, respectively. And E_v, F_v and G_v are the viscous flux vectors. Finally, S_{chem} is a source vector which indicates the rate of formation of chemical species due to the chemical reaction. Each vector is defined as below

$$Q = \begin{bmatrix} \rho \\ \rho u \\ \rho v \\ \rho w \\ \rho e_t \\ \rho Y_i \end{bmatrix}, \quad E = \begin{bmatrix} \rho u \\ \rho u^2 + P \\ \rho uv \\ \rho uw \\ u(\rho e_t + P) \\ \rho u Y_i \end{bmatrix},$$

$$F = \begin{bmatrix} \rho v \\ \rho uv \\ \rho v^2 + P \\ \rho vw \\ v(\rho e_t + P) \\ \rho v Y_i \end{bmatrix}, \quad G = \begin{bmatrix} \rho w \\ \rho uw \\ \rho vw \\ \rho w^2 + P \\ w(\rho e_t + P) \\ \rho w Y_i \end{bmatrix},$$

$$E_v = \begin{bmatrix} 0 \\ \tau_{xx} \\ \tau_{xy} \\ \tau_{xz} \\ u\tau_{xx} + v\tau_{xy} + w\tau_{xz} - q_x + q_{sx} \\ d_x \end{bmatrix},$$

$$F_v = \begin{bmatrix} 0 \\ \tau_{xy} \\ \tau_{yy} \\ \tau_{yz} \\ u\tau_{xy} + v\tau_{yy} + w\tau_{yz} - q_y + q_{sy} \\ d_y \end{bmatrix},$$

$$G_v = \begin{bmatrix} 0 \\ \tau_{xz} \\ \tau_{yz} \\ \tau_{zz} \\ u\tau_{xz} + v\tau_{yz} + w\tau_{zz} - q_z + q_{sz} \\ d_z \end{bmatrix}, \quad S_{\text{chem}} = \begin{bmatrix} 0 \\ 0 \\ 0 \\ 0 \\ 0 \\ \omega_i \end{bmatrix}.$$

The total internal energy, e_t in Eq. (2) is expressed by

$$e_t = \sum_{i=1}^{\text{NS}} Y_i h_i - \frac{P}{\rho} + \frac{1}{2}(u^2 + v^2 + w^2), \tag{3}$$

$$h_i = h_{fi}^0 + \int_{T_{\text{ref}}}^{T} C_{p_i}\,\mathrm{d}T. \tag{4}$$

Table 1
Flow conditions at the DF chemical laser radial-expansion nozzle exit and D_2 injector

		Nozzle exit		D_2 injector
Mach number		4.5		1.0
Temperature (K)		275.86		250.35
Pressure (Torr)		7.49		200.96
Species	F	0.199	D_2	1.0
Mass fraction	F_2	0.050		
	HF	0.437		
	He	0.314		

The enthalpy term in Eq. (4) is particularly expressed by means of the enthalpy of formation, h^0_{fi} and sensible enthalpy. NS represents the number of chemical species involved in the chemical reactions.

q_{x_i} and q_{sx_i} in the energy equation, and d_{x_i} in the species conservation equations can be denoted by

$$q_{x_i} = -k\frac{\partial T}{\partial x_i}, \tag{5}$$

$$q_{sx_i} = \sum_{j=1}^{NS} D_{jm} h_j C_j \frac{\partial Y_j}{\partial x_i}, \tag{6}$$

$$d_{x_i} = \rho D_{jm} \frac{\partial Y_j}{\partial x_i}, \tag{7}$$

where D_{jm} is the diffusion coefficient of jth chemical species in the gas mixture. q_{x_i} and q_{sx_i} represent the conductive heat flux and the heat generation due to the chemical reaction, respectively. The source vector, S_{chem} will be explained in the following section of the chemical reaction model.

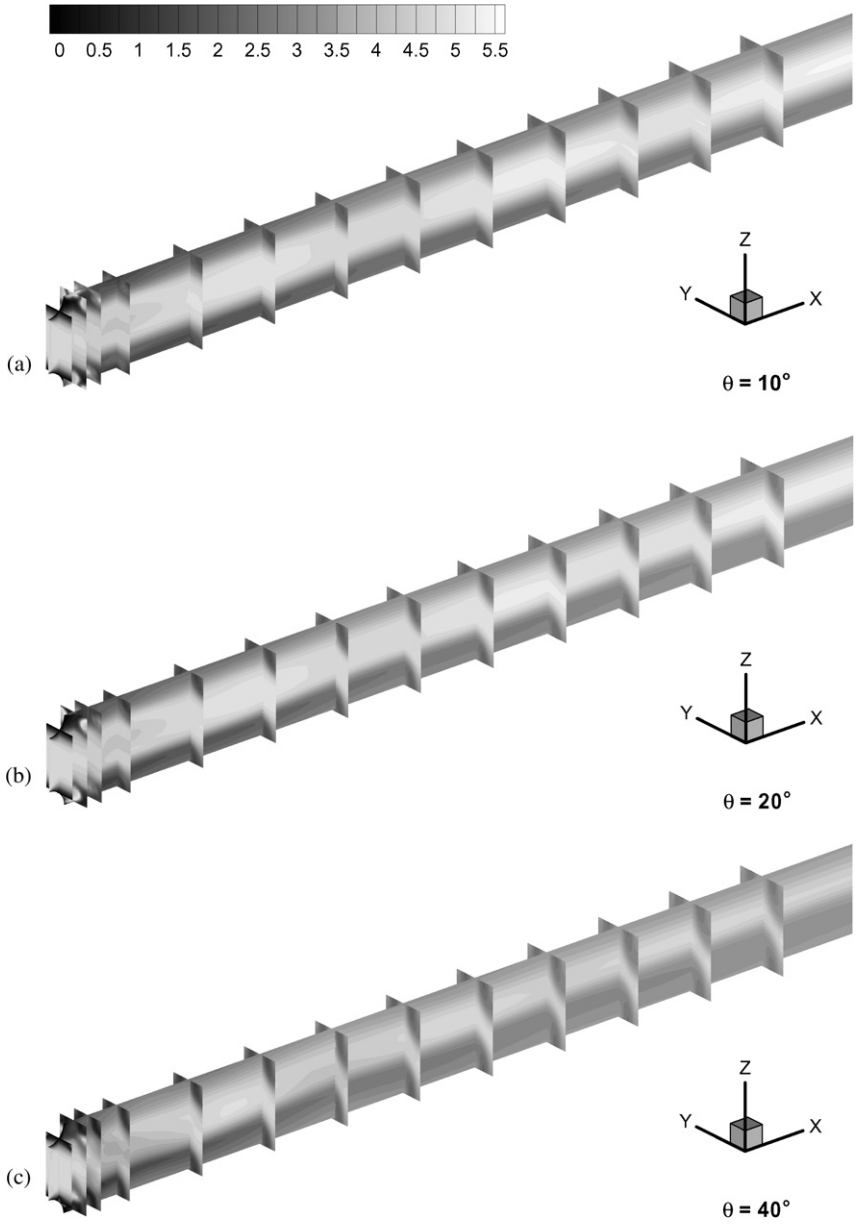

Fig. 3. Effects of D_2 injection angles on the Mach number contours.

In order to close the system of Eq. (2), the equation of state needs to be defined. It is assumed that the macroscopic thermodynamic properties of gas are related through the general equation of state

$$P = P(\rho, e, C_1, C_2, \ldots, C_{NS-1}) = \rho R_u T \sum_{i=1}^{NS} \frac{Y_i}{W_i} = \rho R_u T \left\{ \frac{1}{W_{NS}} + \sum_{i=1}^{NS-1} Y_i \left(\frac{1}{W_i} - \frac{1}{W_{NS}} \right) \right\}. \quad (8)$$

2.2. Chemical reaction model

In order to correctly analyze the population inversion and subsequent lasing power in the chemical laser system, the modeling of the chemical reaction mechanism is important above all. In the DF chemical laser system considered in the present study, the excited DF molecules are created by means of the reaction between D_2 and F, while they are deactivated by collisions, thereby emitting radiation. The chemical reactions considered in the DF chemical laser are as follows:

$$D_2 + F \leftrightarrow \mathrm{DF}(v) + D, \quad v = 0, \ldots, 4, \quad (9a)$$

$$\mathrm{DF}(v) + \mathrm{DF}(v\prime) \leftrightarrow \mathrm{DF}(v+1) + \mathrm{DF}(v' - 1), \quad (9b)$$

$$\mathrm{DF}(v) + M \leftrightarrow \mathrm{DF}(v-1) + M, \quad (9c)$$

$$\mathrm{DF}(0) + M \leftrightarrow D + F + M. \quad (9d)$$

First of all, the excited DF molecules are produced by the pumping reaction (9a). The deactivation by a single quantum jump is governed by vibration–vibration reactions (9b)

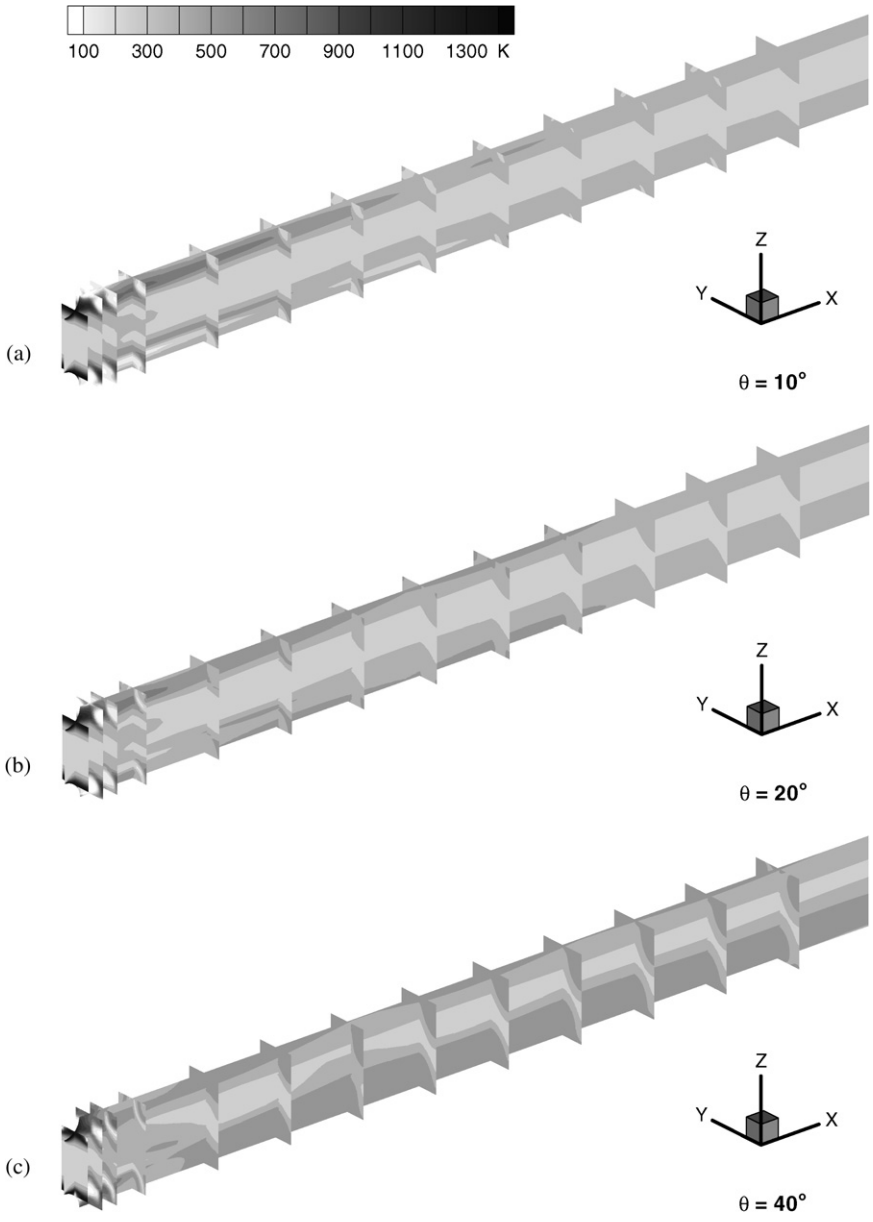

Fig. 4. Effects of D_2 injection angles on the temperature contours.

and vibration–transition reactions (9c). And the dissociation of ground state DF molecules, DF(0) is represented by the reaction (9d) [11].

In order to numerically describe the above chemical reactions, the multi-step chemical reaction model is applied. The rate of change of mass concentration of the jth species is obtained by summing up all the change due to reaction steps mentioned above as follows:

$$\omega_j = W_j \sum_{i=1}^{N_R} \left[\left(v'_{ij} - v''_{ij} \right) \left(k_{fi} \prod_{l=1}^{NS} n_l^{v'_{il}} - k_{bi} \prod_{l=1}^{NS} n_l^{v''_{il}} \right) \right], \qquad (10)$$

where v'_{ij} and v''_{ij} represent the stoichiometric coefficients of the reactants and products for the jth species and the ith chemical reaction step, respectively. n_j is the molar concentration of the jth species, while N_R is the number of the chemical reaction steps. k_{fi} and k_{bi} individually mean the forward and backward reaction rate constants, which are given empirically by the Arrhenius equation.

In the present study, an 11-species (including DF molecules at various excited states of energies) with 32-step chemistry model is adopted for the DF reactions in the DF chemical laser cavity block. A detailed description of the chemistry model can be found in a previous work [12].

2.3. Gain coefficients

All the laser equipments produce laser beam, which has monochromatic, unidirectional and energetic characteristics. The light emitted by a laser is electromagnetic radiation. Therefore, the fundamental equation governing the

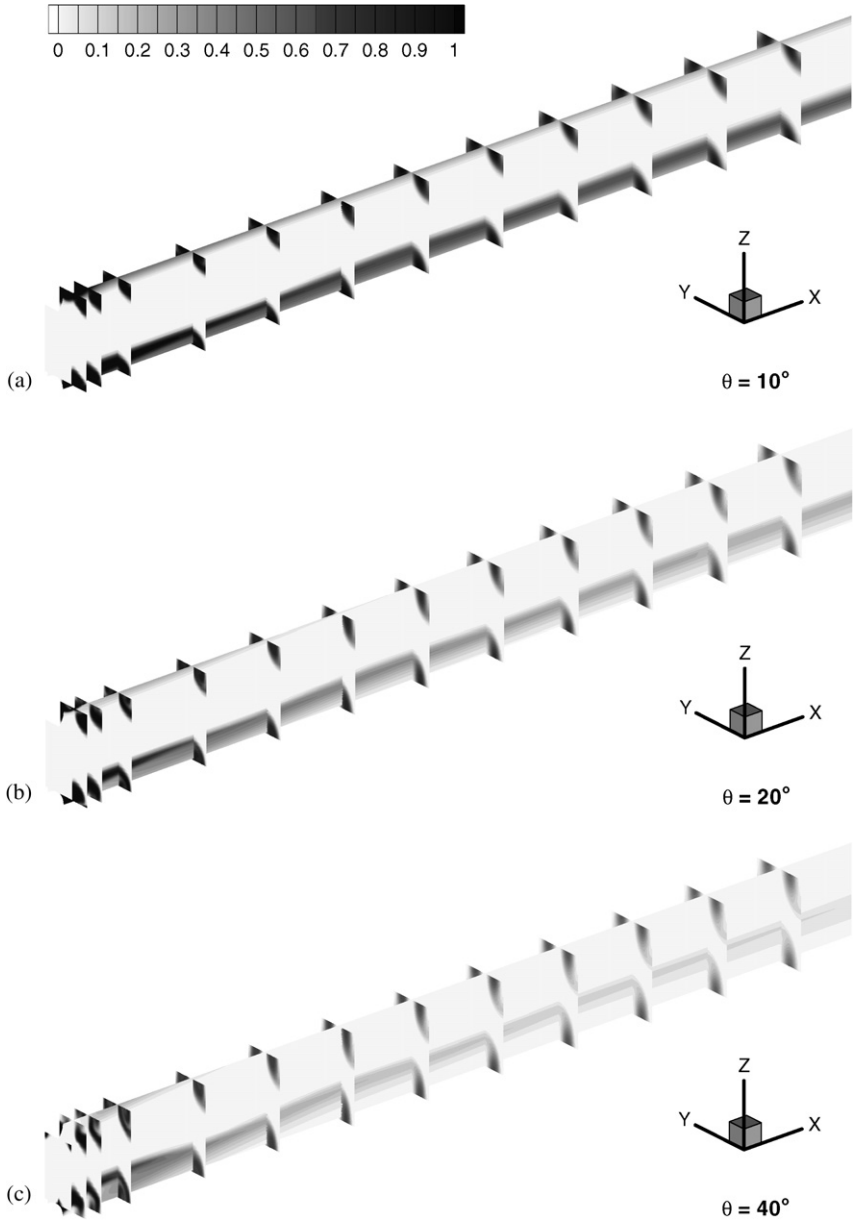

Fig. 5. Effects of D_2 injection angles on D_2 (fuel) mass fraction contours.

electromagnetic radiation within the laser cavity can be written by

$$\pm\frac{\partial I^{\pm}_{v,J}}{\partial z}=\alpha_{v,J}I^{\pm}_{v,J}, \tag{11}$$

where $I^{\pm}_{v,J}$ is the intensity of radiation in the spectral line from $(v+1, J-1)$ to (v,J) propagating in the $\pm z$ direction and $\alpha_{v,J}$ is the optical gain coefficient. For a constant $\alpha_{v,J}$ along the path length, Eq. (11) is integrated to give the Beer's law

$$\frac{I^{\pm}_{v,J}}{I^{\pm}_{0v,J}}=\mathrm{e}^{\pm\alpha_{v,J}(z-z_0)}, \tag{12}$$

where $\alpha_{v,J}$ is positive for gain and negative for absorption. The above equation reveals that the intensity field is remarkably sensitive to the gain or absorption coefficient.

The gain coefficient is calculated with the excited DF molecule concentrations, ρ_v as follows:

$$\alpha_{v,J}=\left(\frac{\hbar N_A}{4\pi W_{DF}}\right)\omega\phi B(v,J)(2J+1)\left\{\frac{\rho_{v+1}}{Q(v+1)}\times\exp\left(-\frac{\hbar c}{\kappa}\frac{E_{v+1,J-1}}{T}\right)-\frac{\rho_v}{Q(v)}\exp\left(-\frac{\hbar c}{\kappa}\frac{E_{v,J}}{T}\right)\right\}, \tag{13}$$

where ϕ is the Doppler broadening line profile function, Q is the rotational partition function for each vibrational level and $E_{v,J}$ is the rotational-vibrational energy at the (v,J) state [13]. And $B(v,J)$ is a matrix related to the Einstein coefficient, $|M^u_l|^2$ which can be expressed by

$$B(v,J)=\frac{16\pi^4}{3\hbar^2 c}\left(\frac{2J}{2J+1}\right)\left|M^u_l\right|^2. \tag{14}$$

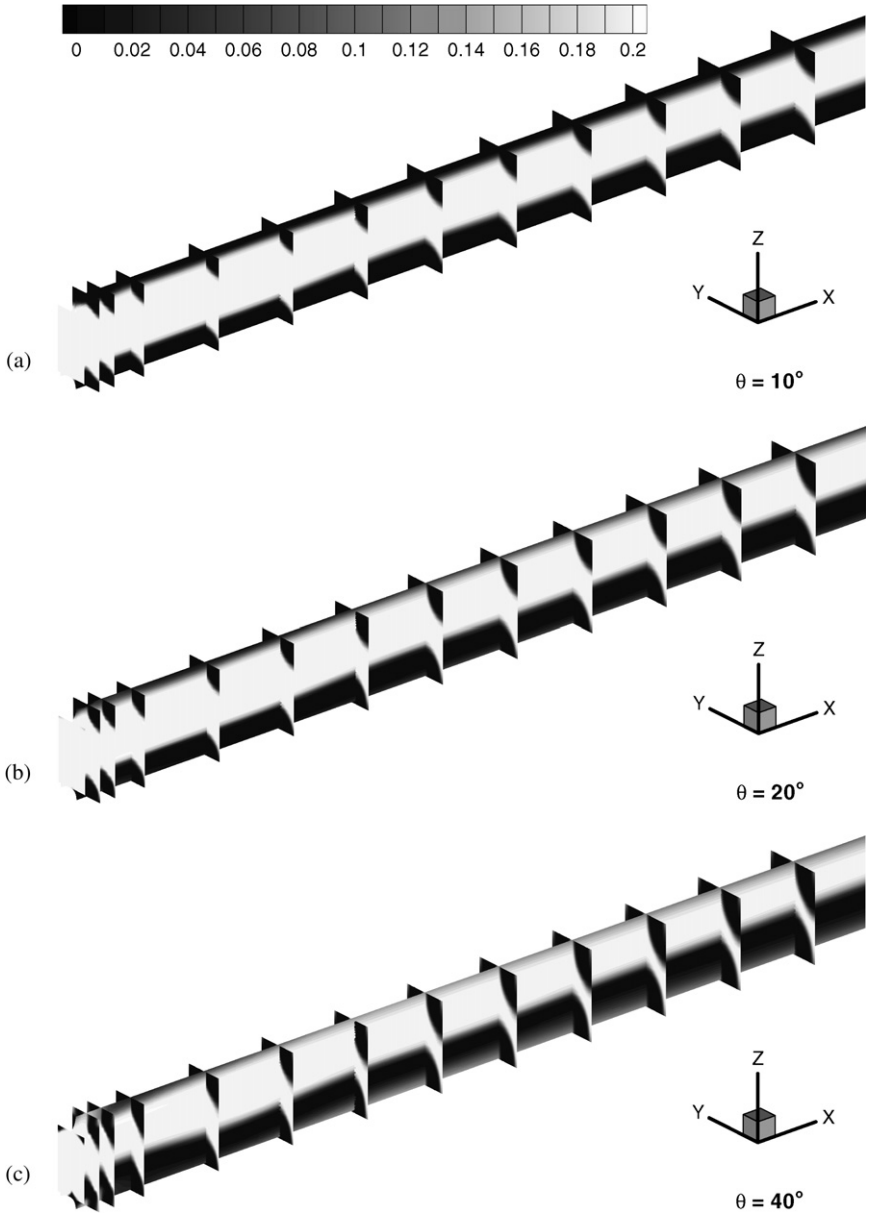

Fig. 6. Effects of D_2 injection angles on F (oxidant) mass fraction contours.

More detailed description of the gain coefficient is given in the handbook of chemical laser [13].

3. Numerical method

In order to analyze the chemically reacting flow field in the chemical laser cavity as illustrated in Fig. 1 and obtain such data for generation of laser beam as species distributions, small signal gains and so on, the governing Eq. (2) have to be simultaneously solved. These equations are the hyperbolic type of equations which are very complicated to solve analytically in the physical domain with complex geometry. Furthermore, a strong shock wave interaction occurs in this region. Therefore the domain is discretized by the finite volume method (FVM) which is known to easily satisfy the conservation rules and to be computationally stable at the surface of discontinuities like shock wave.

First of all, a physical domain is transformed to a computational domain in order to promote the numerical efficiency and conveniently apply the physical boundary conditions using the following coordinate transformation

$$\xi = \xi(x, y, z), \tag{15a}$$

$$\eta = \eta(x, y, z), \tag{15b}$$

$$\varsigma = \varsigma(x, y, z). \tag{15c}$$

After the coordinate transformation, Eq. (2) becomes

$$\frac{\partial \overline{Q}}{\partial t} + \frac{\partial \overline{E}}{\partial \xi} + \frac{\partial \overline{F}}{\partial \eta} + \frac{\partial \overline{G}}{\partial \varsigma} = \frac{\partial \overline{E}_v}{\partial \xi} + \frac{\partial \overline{F}_v}{\partial \eta} + \frac{\partial \overline{G}_v}{\partial \varsigma} + \overline{S}_{\text{chem}}, \tag{16}$$

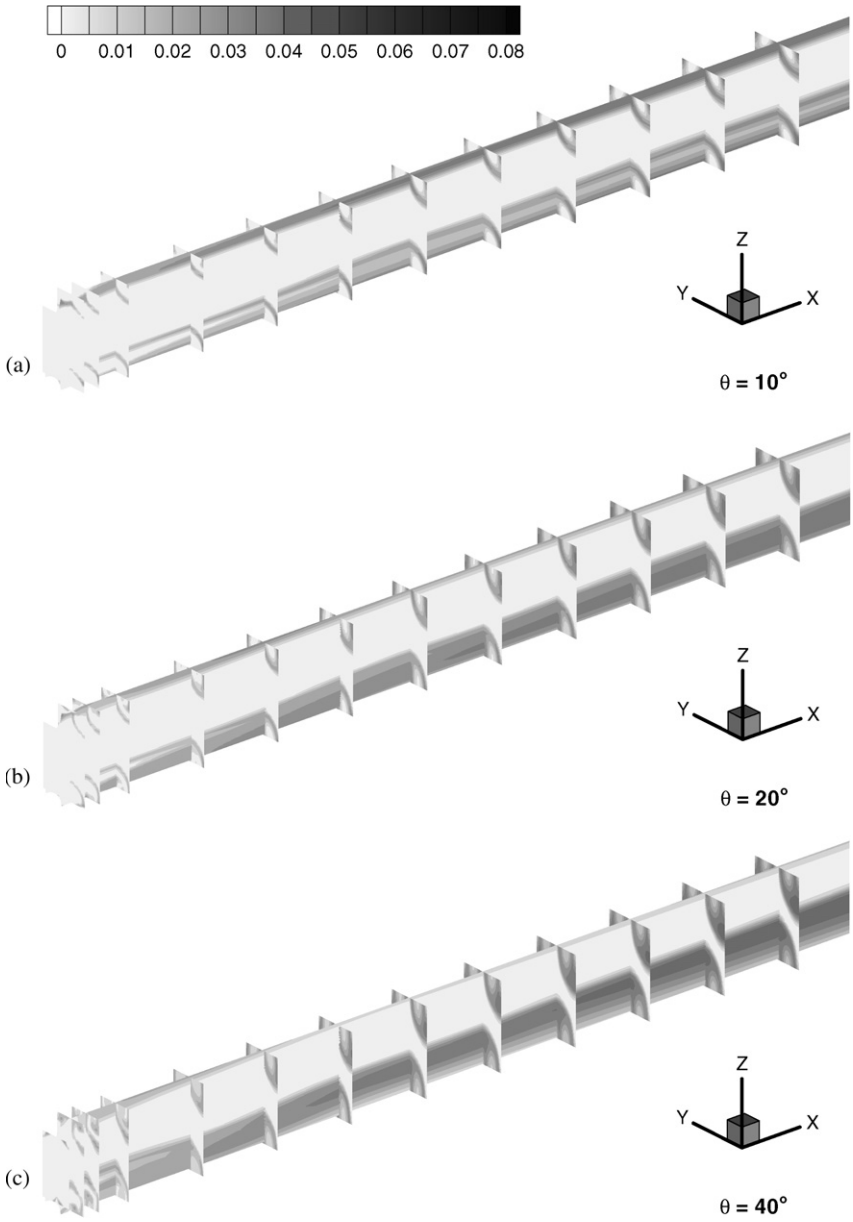

Fig. 7. Effects of D_2 injection angles on the DF(1) mass fraction contours.

where

$$\overline{Q} = \frac{1}{J}Q, \quad \overline{E} = \frac{1}{J}(\xi_x E + \xi_y F + \xi_z G),$$

$$\overline{F} = \frac{1}{J}(\eta_x E + \eta_y F + \eta_z G), \quad \overline{G} = \frac{1}{J}(\varsigma_x E + \varsigma_y F + \varsigma_z G),$$

$$\overline{E}_v = \frac{1}{J}(\xi_x E_v + \xi_y F_v + \xi_z G), \quad \overline{F}_v = \frac{1}{J}(\eta_x E_v + \eta_y F_v + \eta_z G_v),$$

$$\overline{G}_v = \frac{1}{J}(\varsigma_x E_v + \varsigma_y F_v + \varsigma_z G_v),$$

$$\overline{S}_{\text{chem}} = \frac{1}{J}S_{\text{chem}}$$

and Jacobian, J represents the volume of each cell in the Cartersian coordinate system.

The detailed and accurate analysis of shock wave reflection patterns and other shock interactions is achieved by the second-order TVD (Total Variation Diminishing) scheme [14,15]. And van Leer limiter is employed for space discretization of the convection terms and the entropy correction [14,15] is used for $\delta = 0.01$ in order to prevent from occurring the unphysical solutions through the correction of eigenvalues in the flux Jacobian matrix. The viscous terms are discretized by the central difference scheme.

The steady state solution is obtained using the LU decomposition proposed by Jameson and Turkel [16], which has an advantage to reduce the computational efforts in calculating the inverse matrices. And the local time steps are applied for time integration of the governing equations in order to rapidly achieve the numerical solution.

4. Boundary conditions

Fig. 2 illustrates the grid system of a part of the DF chemical laser cavity block which consists of the radial-expansion nozzle exit, round-bended D_2 supply lines, D_2 injection holes and resonator. From the radial-expansion nozzle exit located between two adjacent D_2 supply lines, a supersonic flow radially streams into the laser cavity. Its main constituents are F, F_2, HF and He and are produced in the combustor located upstream for producing F atom. From two injection holes positioned in a staggered way on the round-bended D_2 supply lines located at upper and lower sections, sonic D_2 molecules are injected at angles of 10°, 20° and 40° against the primary flow. The flow conditions at the supersonic nozzle exit and the D_2 injection holes are listed in Table 1, while the adiabatic conditions are applied to the D_2 supply lines except the injection holes.

Whereas the periodic conditions are applied at the upper and lower walls, the symmetric conditions are imposed at the left and right walls, since the flow structure in the physical domain is repeated along the whole nozzle array. At the outlet, the outflow conditions of the first-order extrapolation are used, because the flow exits at the supersonic speed.

The grid system, which is clustered around the D_2 injection holes and near the D_2 supply lines, is constructed with $125 \times 24 \times 41$ nodes after many preliminary calculations with different grid sizes.

5. Results and discussion

A successful control of mixing of D_2 and F is so important to increase a laser intensity level in the DF chemical

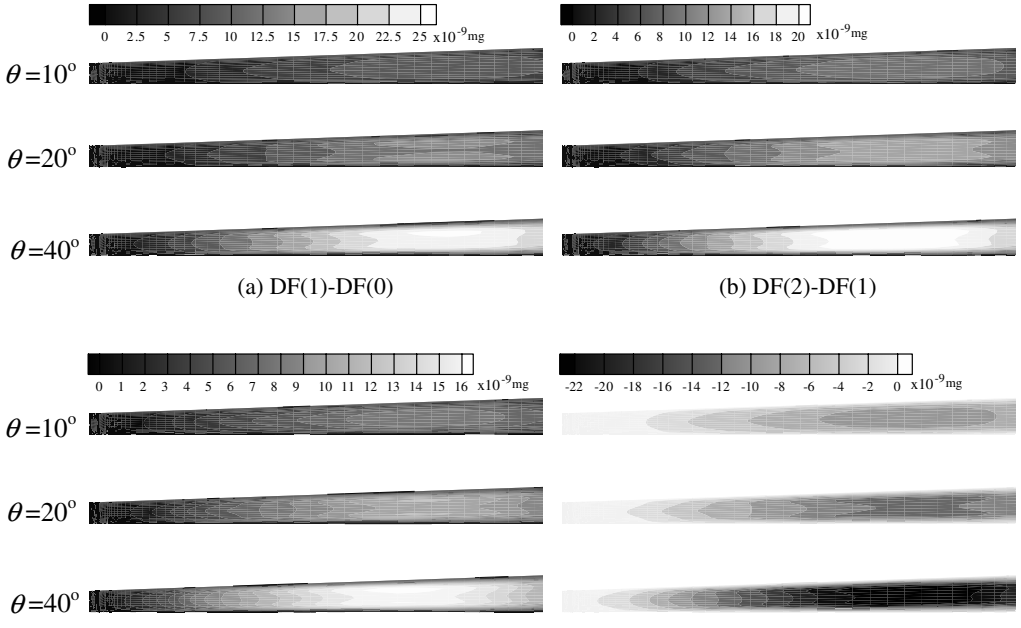

Fig. 8. Effects of D_2 injection angles on the mass ($\int m_{\text{DF}(i)-\text{DF}(i-1)}\,\text{d}z/L$) distributions of DF($i$) − DF($i-1$) in the x–y plane for the cases without lasing.

laser. Unlike other laser systems, the chemical laser has to modulate the mixing rate in order to make the stimulated emission and population inversion strong. Therefore, the characteristics of mixing of a fuel (H_2, D_2, etc.) and an oxidant (F) should be carefully examined for better understanding.

It has been reported that the fuel injection angle against the main steam direction considerably affects the mixing and combustion in the supersonic combustor [17,18]. In the chemical laser cavity which uses a kind of supersonic combustors, the injection angle with the primary oxidant flow ejecting from the radial-expansion nozzle plays an important role of generating excited DF molecules, thereby the population inversion.

Based on the validation of the numerical code for the present study which was already done in the author's thesis work [12], in the following the results calculated with the code developed here would be presented and discussed.

The variations of Mach number with D_2 injection angles are plotted in Fig. 3, which illustrates only a domain in the range of $x = 0$–5 cm. The reason why this limited region is considered is that the resonator with flat mirrors is located in 5 cm length from the nozzle exit.

While the primary mixture of F atom axially flows at the Mach number of 4.0, the D_2 molecules are injected at the Mach number of 1.0 with an angle of 10°, 20° and 40°. Since the Mach number of D_2 molecules is much lower

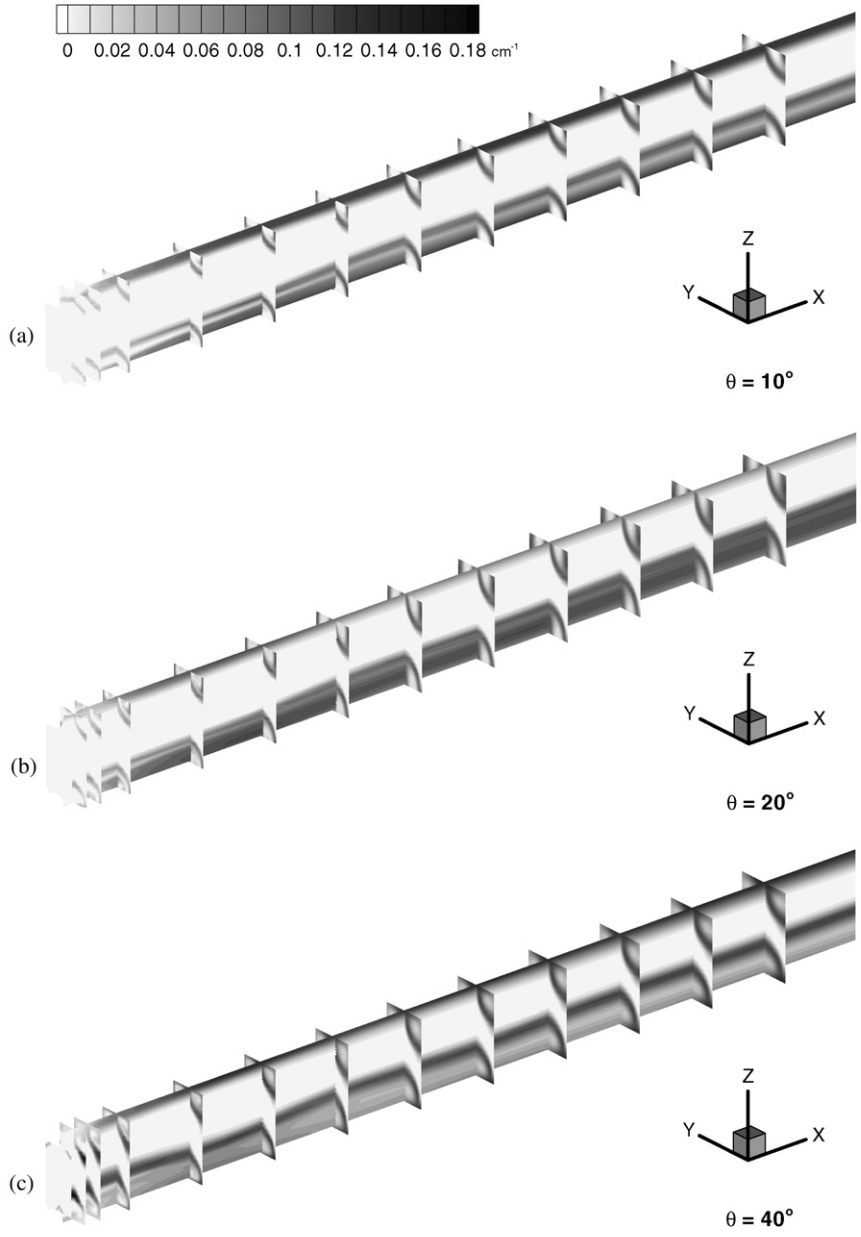

Fig. 9. Effects of D_2 injection angles on the maximum small signal gain contours for the v_{1-0} transition.

than that of primary mixture and their pressure is even higher, as soon as two streams interact, the primary mixture of F atom is decelerated due to low speed of D_2 molecules as shown in Figs. 3a–c. Thereafter, while the D_2 molecules are accelerated due to its interaction with faster primary mixture of F atom, the latter is decelerated along downstream until it meets oblique shock wave. Once the primary mixture meets the oblique shock wave, it is decelerated and then reaccelerated until it meets another reflected shock wave. These phenomena are repeated and clearly observed in Fig. 3a–c. When the D_2 injection angle increases, the degree of deceleration of the primary mixture of F atom becomes severe especially along the center of downstream. In the vicinity of the inlet, a strong interaction of D_2 injection is clearly observed in the figures.

The effects of D_2 injection angles on the temperature distributions are illustrated in Fig. 4a–c. They reveal that the overall temperature increases throughout the whole domain when the D_2 injection angle becomes higher. This result is because of the viscous dissipation of primary flow caused by a high angle of D_2 injection (high penetration), which results from conversion of the kinetic energy to the thermal energy.

The spatial distributions of fuel (D_2) and oxidant (F) with a variation of D_2 injection angles in the DF chemical laser system are given in Figs. 5 and 6, respectively. As the

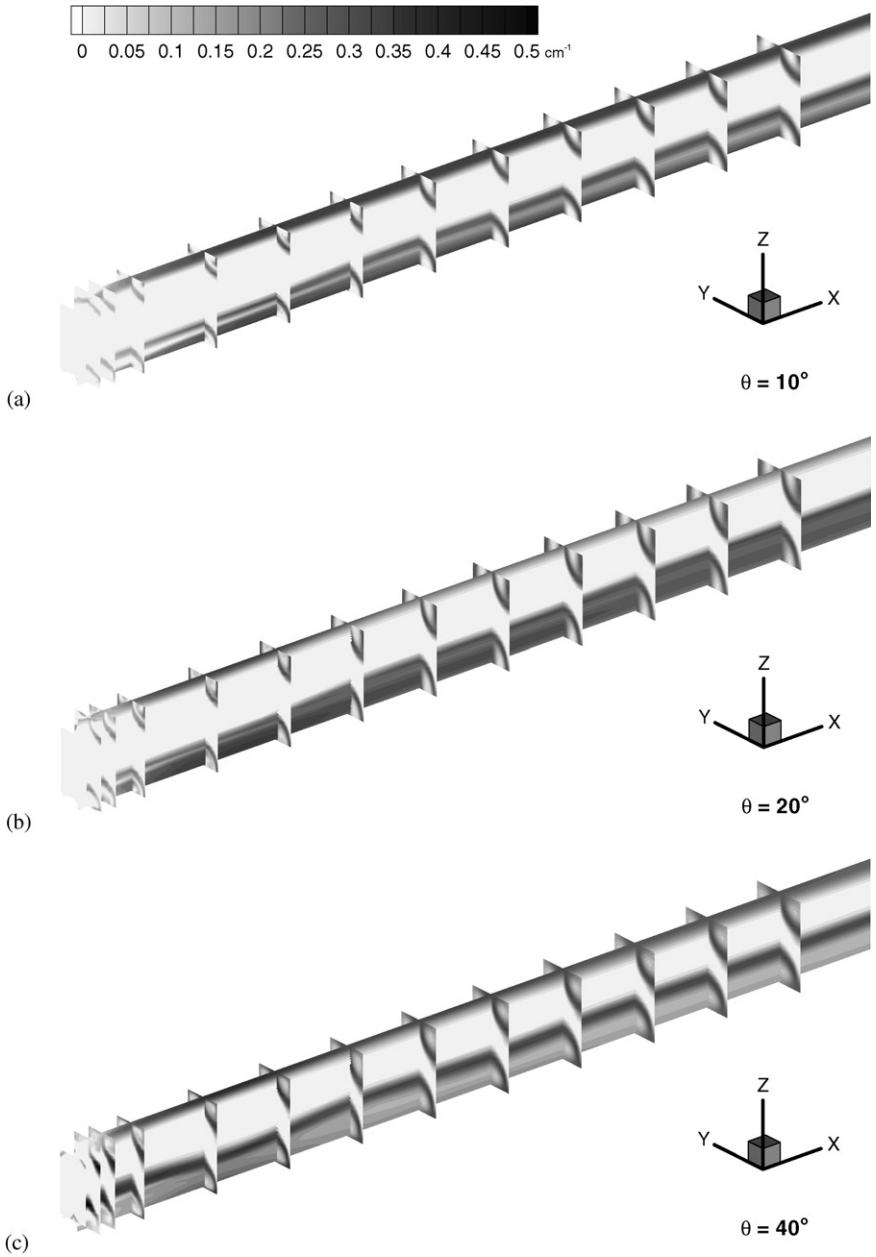

Fig. 10. Effects of D_2 injection angles on the maximum small signal gain contours for the v_{2-1} transition.

D_2 molecules are injected at higher angle with the main flow direction, it is observed that their transverse penetration is deeper, so that the D_2 mass fraction decreases faster as shown in Fig. 5. Instead, as the D_2 injection angle decreases, the D_2 molecules injected at very high pressure spread out farther downstream as illustrated in Fig. 5. Usually, a strong vortex with a horseshoe shape clearly appears near the injection inlet, as the D_2 injection angle increases. This horseshoe pattern is typical of the supersonic injection problems [18,19]. With deeper transverse penetration of D_2 molecules, the rate of reaction of D_2 molecules with F atom becomes higher along the downstream as shown in Fig. 5c. Fig. 6 shows that the F atom as an oxidant is more consumed with an increase in the D_2 injection angle. Therefore, F atom, which is supplied through a supersonic nozzle located at the center of the inlet region, is distributed in narrower center region, as the D_2 injection angle increases. In other words, it is expected that the chemical reaction to produce the excited DF molecules becomes more active with an increase in the D_2 injection angle, which would finally enhance the population inversion in chemical laser.

Fig. 7 represents a variation of DF(1) mass fraction as a representative excited molecule in the DF chemical laser system with D_2 injection angles. The excited DF(1) molecules are observed to be more produced when the D_2 injection angle increases as in Fig. 7c. This is because the higher injection angle of D_2 molecules against atomic F flow direction induces a stronger chemical reaction. It is also

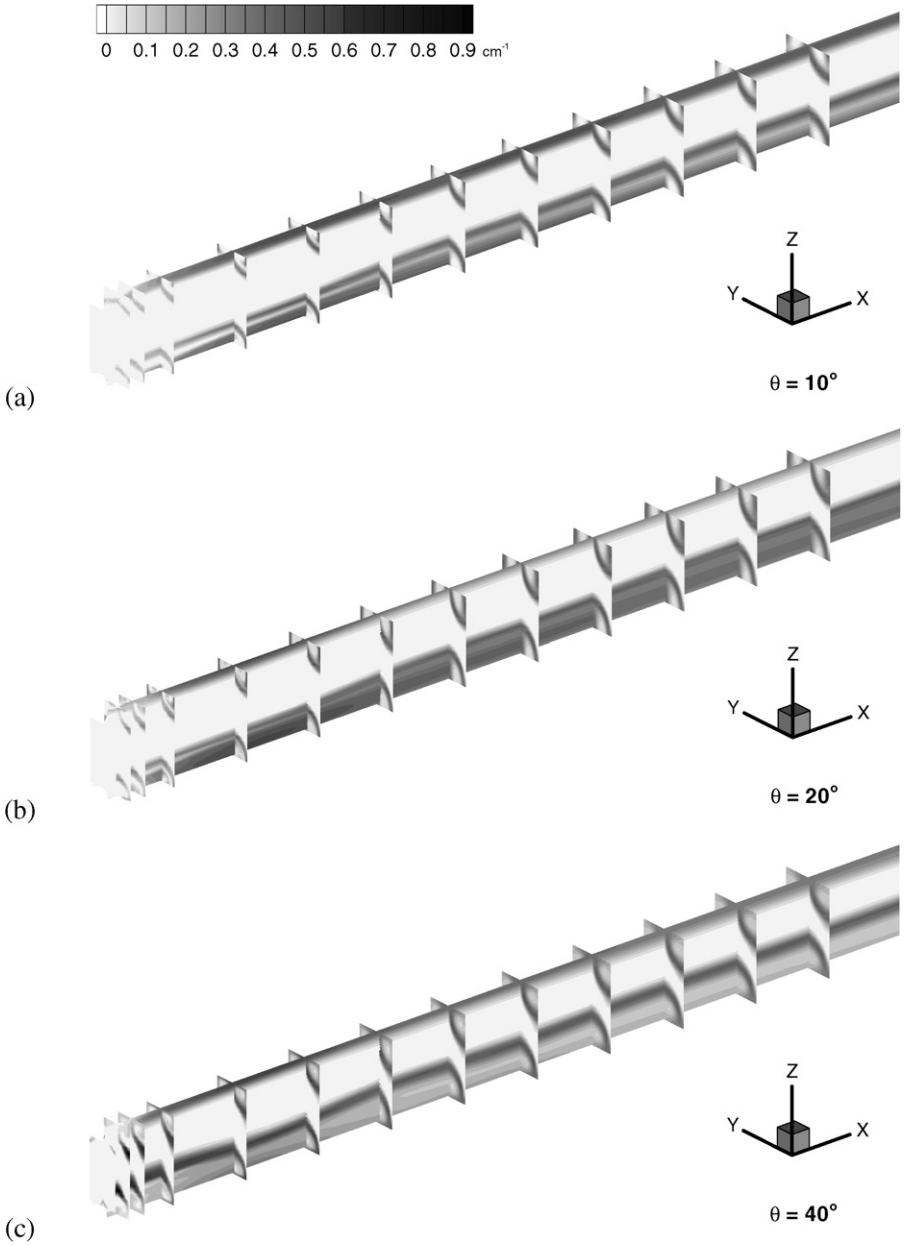

Fig. 11. Effects of D_2 injection angles on the maximum small signal gain contours for the v_{3-2} transition.

noticeable that the production zone of DF(1) molecules of which shape resembles a horseshoe is clearly shown at the top corners in the vertical y–z plane.

Based on the spatial distribution of the DF excited molecules, the differences in each DF excited molecule (DF(i) − DF($i-1$), $i = 1$–4) are illustrated as an indicator of the extent of population inversion in Fig. 8. As the D_2 injection angle increases, all the differences except for the v_{4-3} transition become larger, since chemical reaction as well as mixing becomes larger due to higher D_2 injection angle. In the region of 3–4 cm from the nozzle exit, the difference in DF(i) − DF($i-1$) is maximized. Hence the most intense laser beam may be generated therein. In the v_{4-3} transition, DF(4) − DF(3) becomes negative as shown in Fig. 8d so that this transition is less effective in generating the laser beam than the other transitions.

Figs. 9–12 show the distributions of the maximum small signal gain (SSG) for various vibrational transitions in the resonator. In all vibrational transitions, the highest value of maximum SSG occurs near the inlet when the D_2 injection angle is 40°. As the D_2 injection angle increases, the maximum SSG becomes higher and the volume in which the high gains appear increases. Regarding the v_{4-3} transition as shown in Fig. 12, the maximum SSG along the downstream is observed to be high in wide region, when the D_2 injection angle is equal to 20°. The reason may be deduced from the distribution of DF(4) − DF(3) as shown in Fig. 8. It is said that DF(4) − DF(3) is negative for

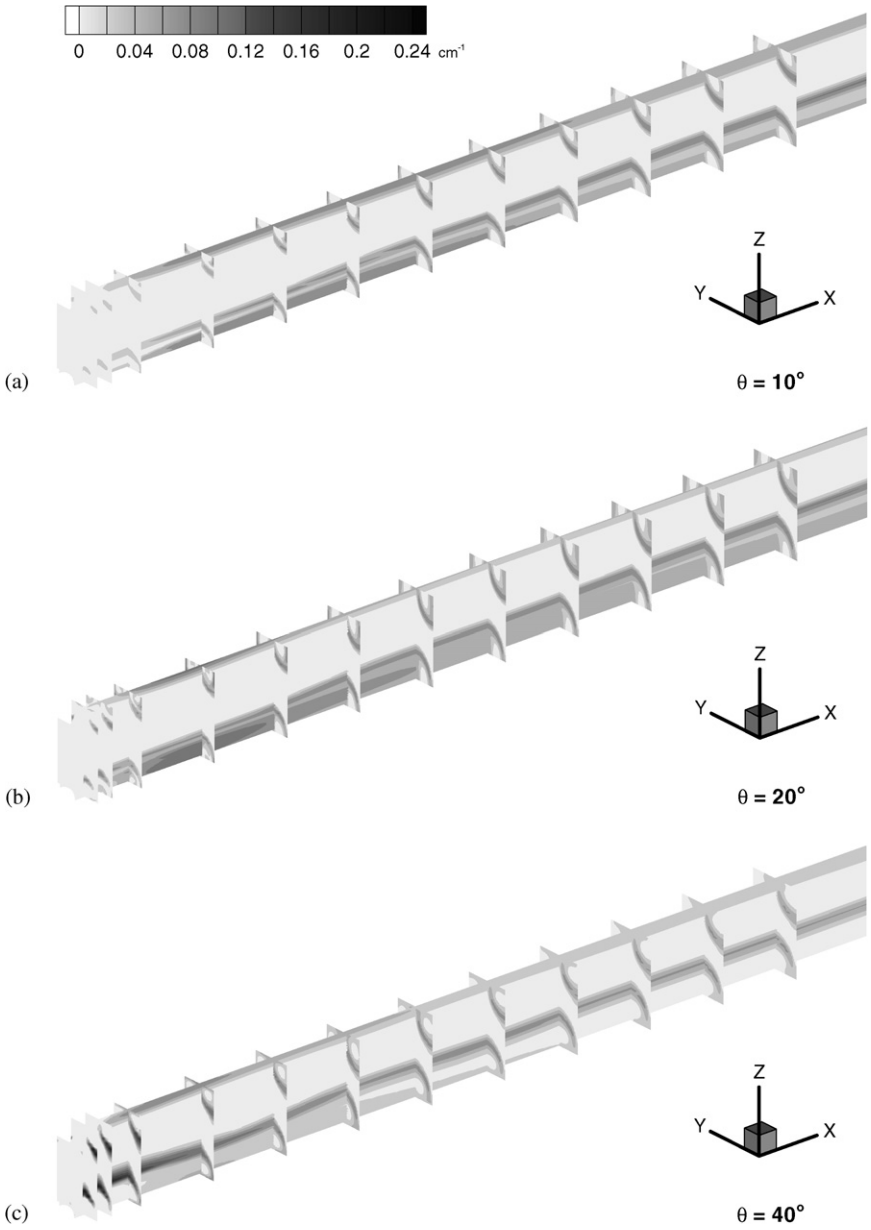

Fig. 12. Effects of D_2 injection angles on the maximum small signal gain contours for the v_{4-3} transition.

$\theta = 40°$ so that the gain coefficient is reduced in this case. The maximum SSG distributions given in Figs. 9–12 reveal that the highest power of laser beam is to be generated when the D_2 injection angle is 40° in this study.

A distribution of the maximum SSG in the x–y plane, which is perpendicular to the optical axis, is shown in Fig. 13. Just in the vicinity of the inlet, the maximum SSG indicate almost zero in all cases. But, except for this region, the maximum SSG becomes maximal for the case of D_2 injection angle of 40°. When the D_2 injection angles are 10° and 20°, the maximum SSG in all vibrational transitions gradually increases along the axial direction. On the other hand, for the case of D_2 injection angle equal to 40°, the maximum SSG increases as far as 2 cm from the nozzle exit, and thereafter, it decreases. These phenomena result from reducing the relaxation time of the DF excited molecules. That is, as the cavity pressure caused by the high D_2 injection angle against the main flow direction increases, the collision of molecules or atoms happens so often that its relaxation time would be reduced. Hence, the region, in which population inversion occurs, becomes narrower as the D_2 injection angle increases. Therefore, the high gain characteristics to locally generate more intense laser beam as well as the relaxation time of the excited molecules should be taken into consideration for better design of chemical laser cavity.

The spatial variation of the static pressure with D_2 injection angles is illustrated in Fig. 14. As the D_2 injection angle increases, the overall static pressure becomes higher in the whole domain. The shock reflection angle also becomes higher, so that the period for its repetition is shorter. Especially, for the case of D_2 injection angle of 40°, the increase in the static pressure is so high that it might be unfavorable to produce the population inversion and the laser beam generate only in the very limited region.

6. Conclusions

An enhancement in chemical reaction as well as mixing efficiency in the supersonic combustor is highly desirable in a development of efficient chemical laser. In this regard, the injection angle formed by two streams of species would play an important role in the chemical laser cavity. A higher injection angle was found to incur strong oblique shock wave and its subsequent reflections in the primary flow so that the field temperature increased highly enough to activate chemical reactions and produce more excited DF molecules. However, so did the static pressure. Consequently, the molecular collision rate related to the whole laser system performance might increase. Regarding the effects of D_2 injection angles in the DF chemical laser system on the population inversion and laser characteristics, the following has been found.

The reaction zone where the DF(1) excited molecules were produced became larger when the D_2 injection angle increased, for the reaction front was larger so that the field temperature turned out to be higher. As the D_2 injection angle increased, the maximum small signal gain became higher and furthermore, the volume in which the high gain appears has also increased. On the other hand, since the collision rate of excited molecules increased and their relaxation time decreased, it counterbalanced the previous favorable conditions for lasing. Consequently, based on these findings, an optimum injection angle is considered to reside at a certain angle

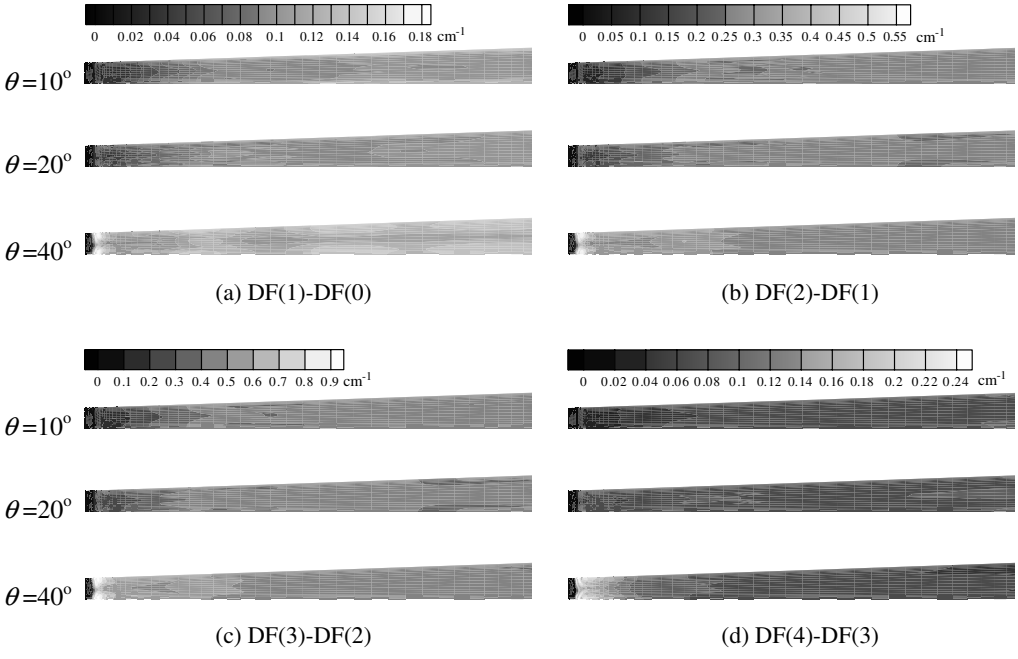

Fig. 13. Maximum small signal gain distributions in the x–y plane.

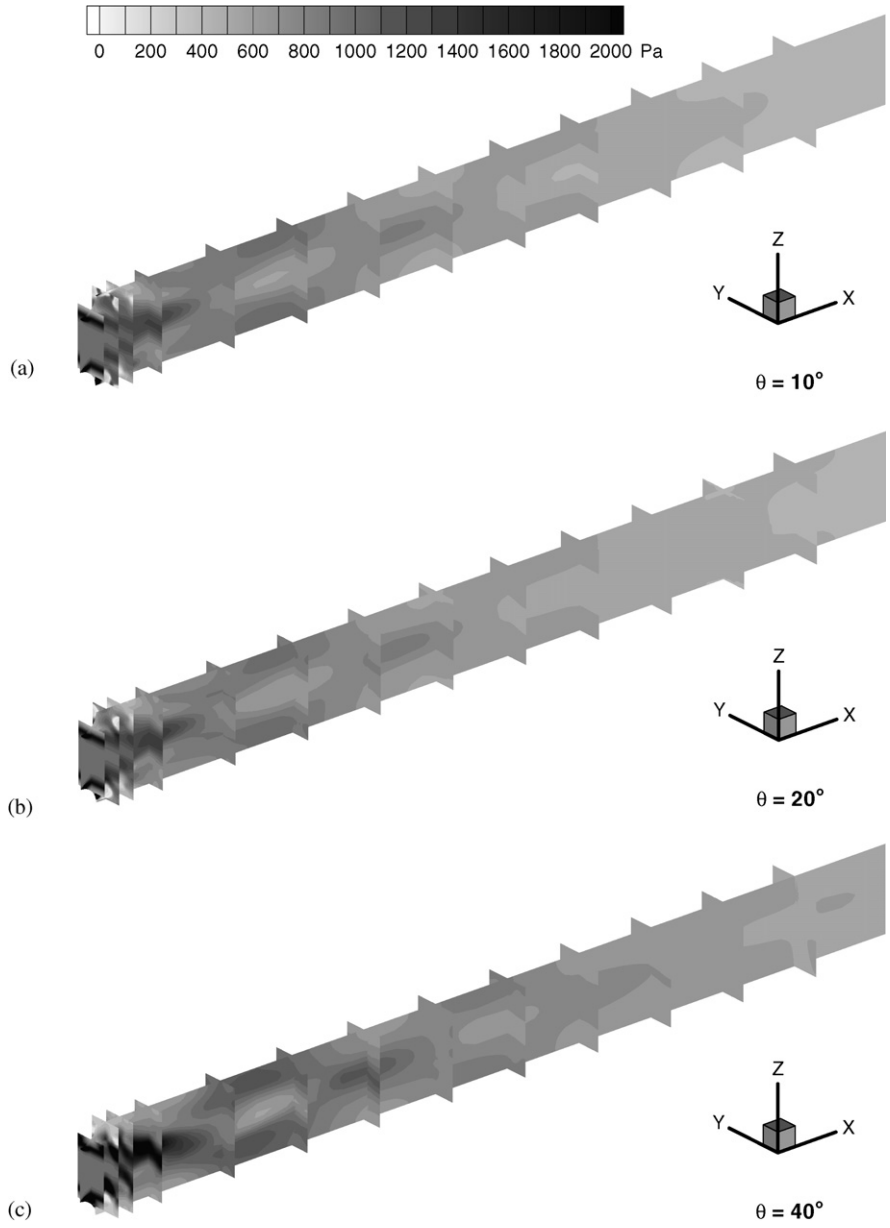

Fig. 14. Effects of D_2 injection angles on the static pressure contours.

between 20° and 40° for positive conditions for the population inversion.

Acknowledgements

This work is a part of the project "Development of Partial Zero Emission Technology for Future Vehicle" funded by the Ministry of Commerce, Industry and Energy. We are very grateful for its financial support.

References

[1] J.S. Park, S.W. Baek, Effects of pressure ratio on population inversion in a DF chemical laser cavity, J. Quant. Spectrosc. Radiat. Transfer 92 (2005) 31–49.

[2] D.J. Spencer, H. Mirels, D.A. Durran, Performance of CW HF chemical laser with N_2 or He diluent, J. Appl. Phys. 43 (1972) 1151–1157.

[3] L.D. Hess, HF chemical laser studies: Use of MoF_6 to increase reaction rates in H_2–F_2 mixtures, J. Appl. Phys. 43 (1972) 1157–1160.

[4] W. Hua, Z. Jiang, Y. Zhao, Nozzle design in CW hydrogen fluoride chemical laser, SPIE 2889 (1996) 135–140.

[5] D.R. Eklund, M.R. Gruber, Study of a supersonic combustor employing an aerodynamic ramp pilot injector, AIAA 99-2249 (1999).

[6] R.P. Fuller, P.K. Wu, A.S. Nejad, J.A. Schetz, Comparison of physical and aerodynamic ramps as fuel injectors in supersonic flow, J. Propul. Power 14 (1998) 135–145.

[7] I.I. Galaev, S.V. Konkin, V.K. Rebone, M.A. Rotinyan, I.A. Fedorov, Calculation and experimental study of the energy and amplifying characteristics of the active medium of a CW chemical HF laser, Quant. Electron. 27 (1997) 290–294.

[8] J.E. Broadwell, Effect of mixing rate on HF chemical laser performance, Appl. Opt. 13 (1974) 962–967.

[9] R.J. Driscoll, G.W. Tregay, Flowfields experiments on a DF chemical laser, AIAA J. 21 (1983) 241–246.
[10] I.I. Galaev, S.V. Konkin, A.M. Krivitskii, V.K. Rebone, M.A. Rotinyan, N.E. Tret'yakov, I.A. Fedorov, Supersonic CW chemical HF laser with a three-jet nozzle array, Quant. Electron. 26 (1996) 211–214.
[11] W.S. King, H. Mirels, Numerical study of a diffusion-type chemical laser, AIAA J. 10 (1972) 1647–1654.
[12] J.S. Park, Study of population inversion and laser beam generation in DF chemical laser system, Ph.D. Thesis, Korea Advanced Institute of Science and Technology, Republic of Korea, 2005.
[13] R.W.F. Gross, J.F. Bott, Handbook of Chemical Lasers, John Wiley and Sons, New York, 1976.
[14] H.C. Yee, Construction of explicit and implicit symmetric TVD schemes and their applications, J. Comput. Phys. 68 (1987) 151–179.
[15] H.C. Yee, A class of high resolution explicit and implicit shock-capturing methods, NASA TM 101099, 1989.
[16] A. Jameson, E. Turkel, Implicit schemes and LU decompositions, Math. Comput. 37 (156) (1981) 385–397.
[17] R.P. Fuller, P.K. Wu, A.S. Nejad, J.A. Schetz, Comparison of physical and aerodynamics ramps as fuel injectors in supersonic flow, J. Propul. Power 14 (1998) 135–145.
[18] L.A. Povinelli, R.C. Ehlers, Swirling base injection for supersonic combustion ramjets, AIAA J. 10 (1972) 1243–1244.
[19] D.R. Eklund, S.D. Stouffer, G.B. Northam, Study of a supersonic combustor employing swept ramp fuel injectors, J. Propul. Power 13 (1997) 697–704.